Scientific Research Publishing

Atmospheric and Climate Sciences, 2025, 15(1), 1-19
https://www.scirp.org/journal/acs
ISSN Online: 2160-0422
ISSN Print: 2160-0414

Calculation of Compound Hazard Probability Using Convolution of Distributions

Luis Augusto Sanabria

Independent Researcher, Melbourne, Australia
Email: lasf1327@gmail.com

How to cite this paper: Sanabria, L.A. (2025) Calculation of Compound Hazard Probability Using Convolution of Distributions. *Atmospheric and Climate Sciences*, **15**, 1-19.
https://doi.org/10.4236/acs.2025.151001

Received: September 24, 2024
Accepted: November 24, 2024
Published: November 27, 2024

Abstract

The hazard produced by natural phenomena on infrastructure and urban populations has been widely studied in the last 50 years. Researchers have recognised that the real danger posed by these phenomena depends on their extreme values. Most researchers focus on the extremes of natural phenomena considered in isolation, one variable at a time. However, what is relevant in hazard studies is coincident extremes of several climatic variables, i.e., the presence of compound extremes. The peak value of these extremes seldom coincides, but off-peak values located in the tail of the distributions are often concurrent and can lead to catastrophic events. What is essential in hazard studies is to calculate the probabilistic distribution of the extremes of coincident climatic variables. The presence of correlations between these variables complicates the problem. This paper presents a computationally efficient and robust mathematical methodology to solve the problem. The procedure is based on the convolution of the distributions of the climatic variables. Once the probabilistic distribution of the compound variables is found, it is possible to calculate the curves of the return period, which is the indicator of importance in hazard and risk studies. This compound Return Period is computed using the Statistics of Extreme Values. To illustrate the problem, the case of a cyclone landing close to a low-gradient coastal city is discussed, and its probability of flooding and recurrence period is calculated. We show that the failure to correctly model the correlation between variables can result in overestimating the Return Period curve, consequently increasing mitigation costs.

Keywords

Natural Hazards, Compound Extremes, Mathematical Convolution

1. Introduction

The hazard produced by natural phenomena on infrastructure and urban

populations has been widely studied for the last 50 years. Researchers have recognised that the real danger posed by these phenomena depends on their extreme values [1]-[6]. The study of extremes of natural phenomena was boosted with the development of the Statistics of Extreme Values in the 1950s. This branch of mathematics allows the analyst to study extremes of natural phenomena in a systematic way [7]-[9].

Most researchers focus on the extremes of natural phenomena considered in isolation, one variable at a time. However, what is relevant in hazard studies is the coincidence of extremes of several variables, *i.e.*, the presence of compound extremes. In general, compound extremes of climatic variables are defined as concurrent or coincident extremes of multiple variables in a given region at a given time. Compound extremes may exacerbate an already dangerous situation, leading to a more significant impact on humans and the built environment than extremes of single variables [10]-[13]. Often, the combination of extremes increases the hazard; [14] and [15] show that if severe winds destroy the roofs of buildings, the concurrent heavy rain causes more damage. In some situations, the value of a single variable is not dangerous in itself, but the combination of several climatic events could give rise to an extreme event. [16] show that traditional univariate risk assessment substantially underestimates the risk of extreme events such as the 2014 California drought because of ignoring the effect of temperature. [17] show that the drought that occurred in Europe in 2003 was not the most severe in the continent; however, in combination with extended heatwaves and wildfires, it is considered the most fatal, with more than 70,000 people dying as a result of these extreme conditions.

In other cases, the problem itself depends on several extremes of climatic variables, such as the study of coastal erosion due to sea storms, which depend on wave height, wave period, storm duration, wave direction, water level and storm-interarrival time [18]. Wildfires, a severe problem in south-eastern Australian states, depend on high-temperature values, wind speed and drought; the latter is defined as extremes of low precipitation. If, together with these climatic variables, there is also a lot of fuel in a given region (in the form of dry grass), there is a high probability of a wildfire developing in the region [19]-[21].

Failure to model compound events correctly results in an inaccurate assessment of the hazard, with severe consequences for the infrastructure. [22] show that considering the compound effect of sea-level rise, groundwater inundation, and precipitation flooding, the drainage capacity of a coastal watershed in California (USA) will be breached, and a large region will be flooded, whilst the univariate model fails to recognise the danger. Similar results are reported by [23].

One limitation of most compound hazard models is that they do not assess the probability of concurrent extremes occurring. In some cases, this probability is too low, and the possible impact of these phenomena can be neglected with savings for the planning authorities. In other cases, the likelihood of concurrent events happening is significant, especially considering future climate conditions

and must be included in the model [24]-[26].

What is essential in all these cases is to calculate the probability that two or more extreme values of climatic variables, not necessarily their peak values, occur concurrently, [27] studied the impact of typhoons, rainfall, and storm surges, three correlated variables produced by the landing of a cyclone. Floods quickly occur in coastal cities when cyclones land in these regions, often bringing heavy rainfall and storm surges. They model the phenomenon using a trivariate joint probability distribution of the three elements: typhoon landing, rain and storm surge. The joint probability distribution can quantify the probability that extremes of multiple variables arise simultaneously.

Modelling multivariate extremes is more complicated than the single-variate case. In particular, in the former, it is necessary to consider the correlation between variables; in most cases, the assumption of independence that underpins the single variate case is no longer applicable [15] [28]-[30].

In general, there are two methodologies to model multivariate extremes; one is by using a multivariate extreme value distribution [1] [31]-[34], and the other is by performing the convolution of the individual random variables to obtain the distribution of the combined variables. The latter case can be greatly simplified because the combined distribution can be analysed using the tools of the univariate case [35].

This study uses the latter methodology: it convolves the individual random variables to obtain the combined random variable. The convolution is performed using the method of cumulants [36] [37]. The tail of the distribution of the combined random variable determines the extreme behaviour of the combined distributions, and this tail can be modelled using the Statistics of Extreme Values. In particular, we present a flexible, efficient methodology to calculate the probability that compound extremes of "n" random variables of natural phenomena occur, considering the possible correlation between these random variables.

This probability can be transformed into an Average Recurrence Interval (ARI), the indicator of importance in hazard and risk studies [1] [28] [38]. The ARI termed Return Period (RP) in engineering studies allows the planner to calculate the magnitude of extreme values of natural phenomena and the frequency with which these values repeat.

The paper's layout is as follows: Section 2 presents the mathematical basis of convolution. Section 3, discusses the method of cumulants to calculate the curves of RP of compound events using the convolution of distributions. Section 4 presents an example problem to illustrate the methodology, and Section 5 analyses the results.

2. Mathematical Convolution

The combination of the distributions of several random variables (rvs) is termed a mathematical convolution. In the general case, the operation gives rise to complex integrals that are difficult to solve analytically. In practice, the solution is achieved

using transformations [39] [40] or numerical methods [37] [41]. To illustrate the process, consider two simple examples: In the first one, we will convolve the discrete distributions of two independent random variables X_1 and X_2. In the second example, we convolve two independent Normal distributions $N_1\left(m_1, \sigma_1^2\right)$ and $N_2\left(m_2, \sigma_2^2\right)$. The convolution of two independent Normal distributions is an easy operation because Normal distributions have the reproductive property, *i.e.* the combination of two Normals produces another Normal with parameters (m_1 + m_2) and ($\sigma_1^2 + \sigma_2^2$).

2.1. Convolution of Discrete Distributions

For the first case, consider the distributions of wind speed in m/s recorded at two independent weather stations. The discrete distributions of the rvs, called X_1 and X_2, are shown in **Figure 1**. The distribution of X_1 has only two impulses (0.3, 0.7) located at (3, 5). The distribution of X_2 has 3 impulses (0.2, 0.6, 0.2) located at (3, 6, 8). The convolution of both rvs, X_1 and X_2, is defined as

$$Z = X_1 + X_2 \tag{1}$$

and is performed numerically by adding together the x-axis and multiplying the corresponding probabilities, as shown in **Figure 1** (bottom). The convolution, in this case, implies shifting the distribution to the right and reducing the size of the impulses. The realisation of events X_1 = 5 m/s and X_2 = 6 m/s occurring concurrently is given by

$$P[Z=11] = P[X_1 = 5 \mid X_2 = 6] = P[X_1 = 5]P[X_2 = 6] = 0.42 \tag{2}$$

to stress the point, **Figure 1** shows the x-axis of the individual rvs below the main x-axis. Discrete distributions have been used to model landslide hazard [42].

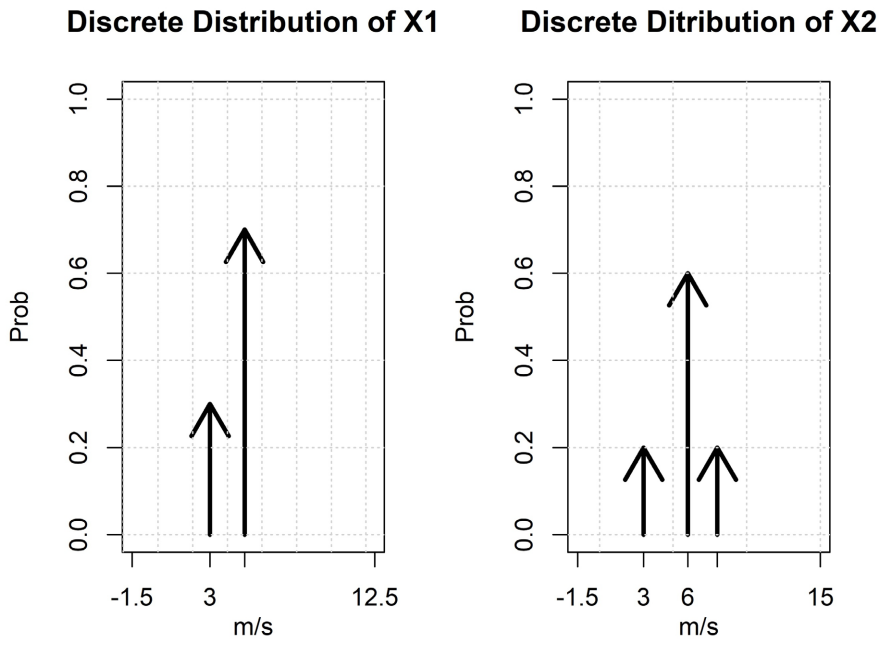

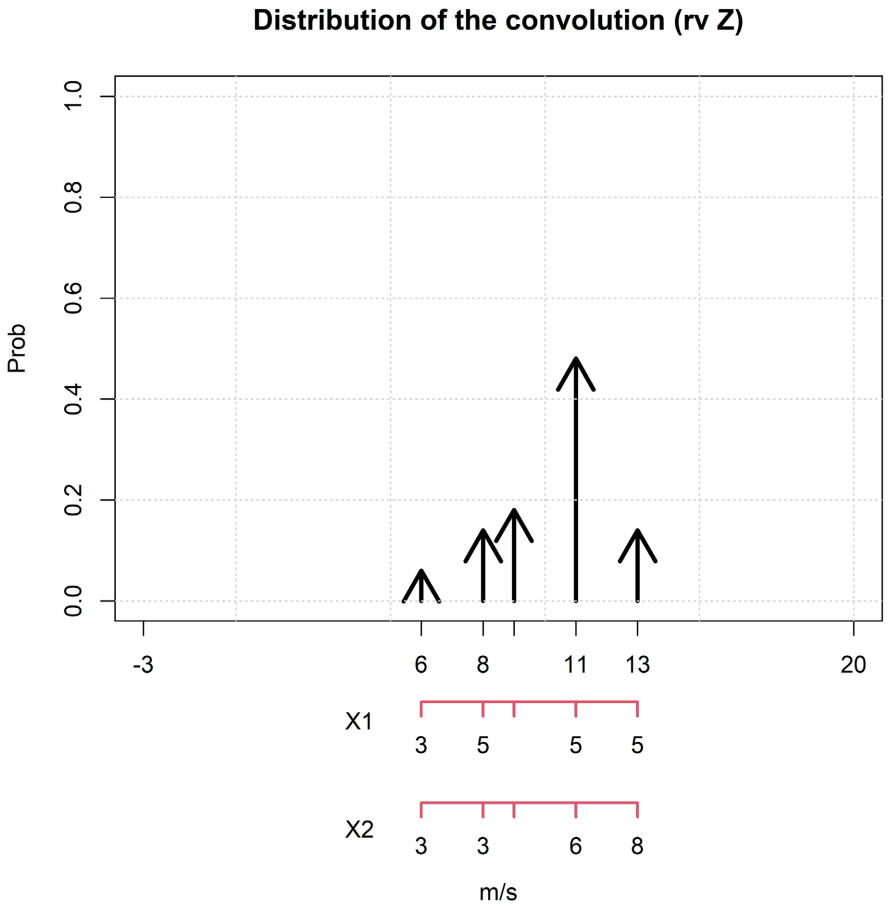

Figure 1. Convolution of two discrete distributions.

2.2. Convolution of Continuous Distributions

The independent Normal distributions are shown in Figure 2. The parameter of Normal 1, N_1 (blue curve), are (2,1), *i.e.* mean (m_1) = 2 m/s, and Variance (Var) = 1 (m/s)^2. The parameters of Normal 2, N_2 (red curve), are (3.5, 0.25). The corresponding convolution is a Normal with parameters (5.5, 1.25). Again, observe that the net effect is a shifting of the resulting distribution (black curve) to the right and a reduction of the body of the distribution (because of the combination of probabilities). In this case, showing the combination of the individual x-axis is more challenging because the distributions are continuous. Still, as in Figure 1, we show a few points of the original distributions below the main *x*-axis.

The equivalent to Equation (2) in continuous distributions requires the cumulative distribution function (CDF) shown in Figure 3. In this case, the probability of events $N_1 < 3$ m/s and $N_2 < 4$ m/s occurring simultaneously is given by

$$P[Z<7]=P[N_1<3 \mid N_2<4]=P[N_1<3]P[N_2<4]=0.91 \quad (3)$$

[41] and [37] present more examples of convolutions.

In risk analysis, we are more interested in the complementary event $P[Z>z_1]=1.0-P[Z<z_1]$.

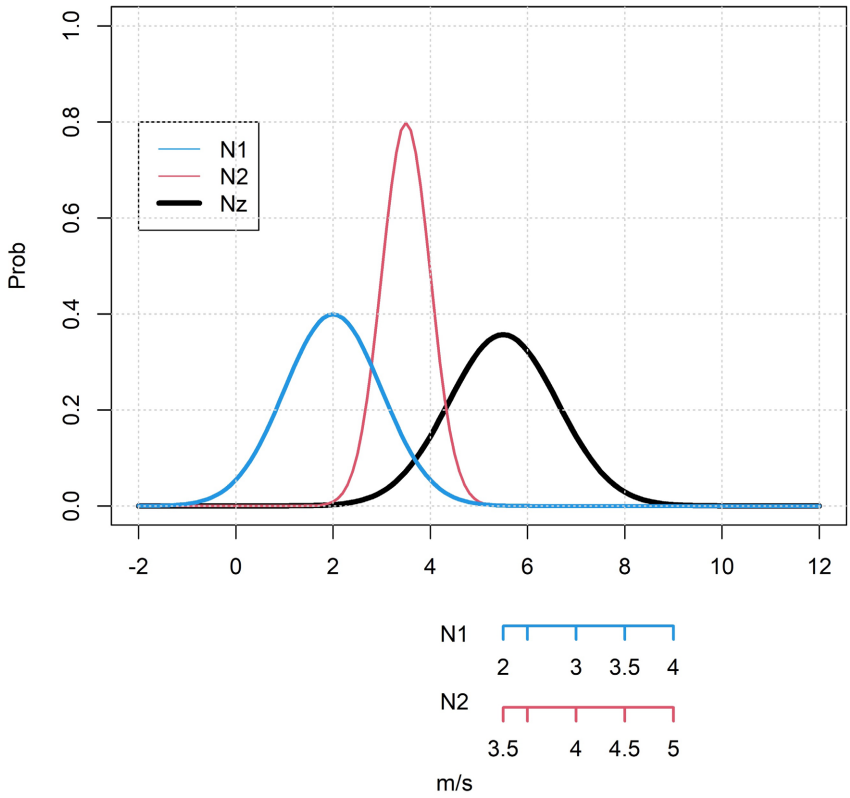

Figure 2. Convolution of continuous distributions.

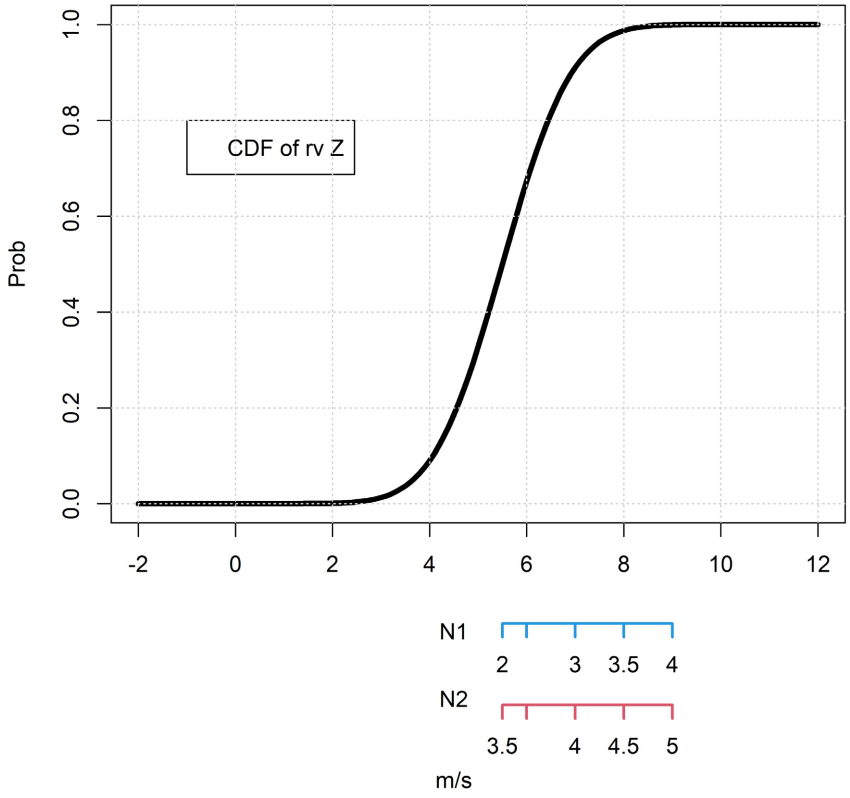

Figure 3. Distribution Function of rv *Z*.

If z_1 is large, we are selecting the extreme values of Z, our compound variable. The value $P[Z > z_1]$ represents the probability that the concurrent extremes of N_1 and N_2 are exceeded. The hazard and risk studies of natural phenomena aim to calculate the frequency with which extreme values repeat. As mentioned before, the main indicator in these types of studies is the Return Period (RP). A curve of RP shows the recurrence of extreme values, usually in years, at a given region. These extreme values are termed Return Levels. Thus, if the 50-year RP of wind speed at a given region is 30 m/s, what we are saying is that 30 m/s is expected to be exceeded, on average, once every 50 years.

The curve of RP can be built from **Figure 3** ([1] [2]), using the expression,

$$\mathrm{RP} = \left(1.0 \Big/ \left(1.0 - P[Z < z_1]\right)\right) \Big/ \mathrm{nopy} \tag{4}$$

where RP is the Return Period corresponding to the z_1 Return Level. The constant "nopy" sets up the right scale for the curve and depends on the physical characteristics of the problem.

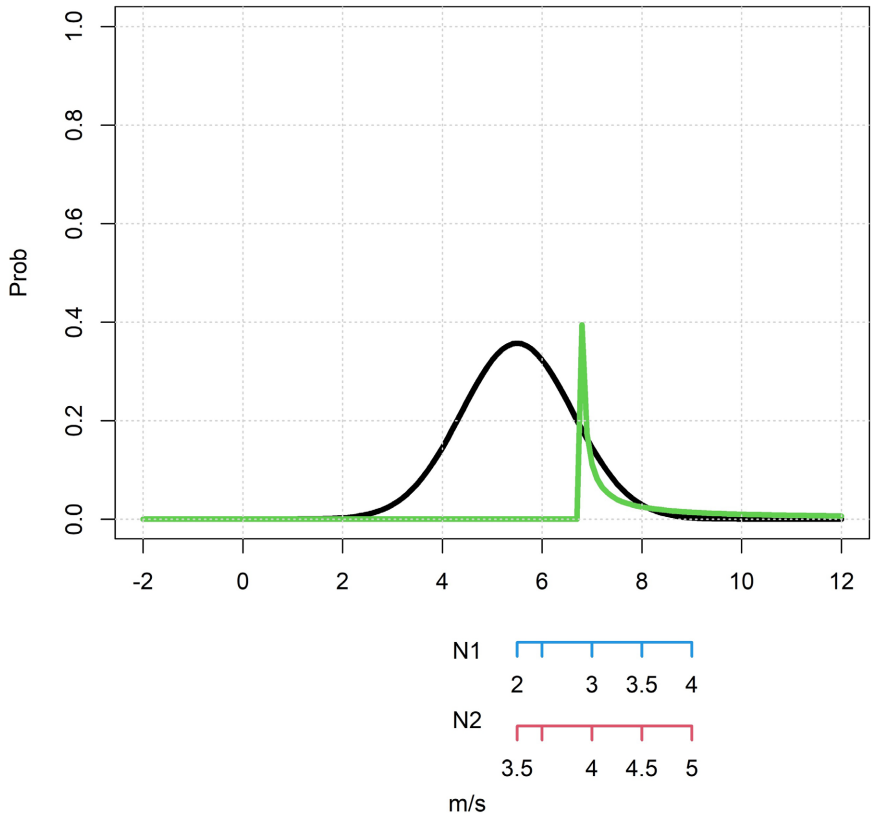

Figure 4. Fitting the GPD to the tail of the Compound distribution.

The major limitation of this technique is that it allows us to calculate RPs for the same period of the given data, usually 20 or 30 years. In practical problems we are interested in calculating RP for values well beyond the available data. The Australian/NZ regulations [43], for instance, prescribe wind loads for design of structures corresponding to return periods of 500 years. In this case we should use

extreme value distributions to extrapolate RPs to 50, 100, 500 years and beyond. The technique consists in fitting an extreme value distribution to the tail of the distribution of the compound variable (black curve in **Figure 2**). There are a number of families of extreme value distributions available to do this, in our example we will use the Generalised Pareto distribution (GPD), and we will fit the GPD using the method of moments [44] [45]. **Figure 4** shows the fitting of the GPD to the tail of the compound extremes (green curve). From the parameters of the GPD we can calculate the parameters of the RP curve, as will be explained in Section 3.2.

More information has to be provided to calculate the curve of RP. Suppose that the Normal distributions of **Figure 2** refer to the maximum daily wind speed (m/s) recorded at two independent stations in Australia. The records cover a period of 20 years for each station; hence the convolution of the two distributions refers to a period of 40 years. Furthermore, suppose that the maximum value found in the records for each Normal distribution is 5.5 and 6.5 m/s, respectively. The maximum of the combined distributions will be 12 m/s. Hence, we can say that the 40-year RP of max daily wind speed at the region is 12 m/s, the correct scale to use in Equation (4) is nopy = 9.44. **Figure 5** shows the corresponding curve of RP. From this curve, we can say that the combined events, wind speed at station 1 = 5.5 m/s and wind speed at station 2 = 6.5 m/s occur, on average, once every 50 years, as shown by the scales to the left of the *y*-axis.

Note that this is just an example; in practice, it is inappropriate to fit Normally-distributed data with extreme value distributions [2].

3. Methodology to Calculate Curves of RP of Compound Events

This paper aims to present an efficient methodology for calculating curves of RP of compound events. This methodology is based on the method of cumulants to convolve any number of independent rvs. The technique can easily be extended to the case of non-independent rvs, as we will see later.

3.1. Convolution Using the Method of Cumulants

In this method, the rvs are replaced by a set of parameters called cumulants. These cumulants are linear combinations of the moments of the distribution. The convolution consists on adding together the cumulants of the components to obtain the cumulants of the resulting distribution. From these cumulants the distribution of the resulting rv can be calculated [37]. Consider the linear equation,

$$Z = aX + bY + c \tag{5}$$

where,

a, b, c = constants.

X, Y = Independent random variables.

Z = Resulting random variable.

Let m_x and m_y be the mean of X and Y; and let $\kappa_r(x)$ and $\kappa_r(y)$ be the cumulants of X and Y respectively. The subscript "r" indicates the order of the cumulant.

In terms of moments and cumulants Equation (5) can be expressed as,

$$m_z = am_x + bm_y + c \tag{6}$$

$$\kappa_r(z) = a^r \kappa_r(x) + b^r \kappa_r(y) \quad \text{for cumulants of order } r > 1 \tag{7}$$

Note that the operation does not involve any approximation. Equation (6) and (7) can be collapsed into one [37].

One of the strengths of the method of cumulants for convolution of rvs is that the process can easily be extended to the case of non-independent rvs, *i.e.* for the case in which there is some degree of covariance between the rvs. The covariance indicates whether both variables follow the same pattern of change. If X tends to increase or decrease along with Y, the covariance will be large and positive. If, on the other hand, X tends to increase as Y decreases their covariance would be a large negative number.

Let us suppose that the covariance between the rvs X and Y is σ_{xy}, then the second cumulant or Variance of rv Z has to be modified to take this covariance into account. Equation (7), then, becomes,

$$\kappa_2(z) = a^2\kappa_2(x) + b^2\kappa_2(y) + 2ab\sigma_{xy} \tag{8}$$

3.2. Curves of RP

There are basically two techniques to calculate the RP. One is the so-called "block maxima" in which an extreme value distribution is fitted to the annual maxima. The distribution used in this case is the Generalised Extreme Value Distribution (GEV). If more observations are available, for instance, maximum daily observations, "block maxima" is not recommended because it uses only one observation per year; the other observations are not used, which may result in a poor fitting of the data. The second technique is the "peaks-over-threshold". This technique utilises all values over a given threshold to fit the distribution. In this case, the Generalised Pareto Distribution (GPD) is used. This methodology has several advantages over the "block maxima" method; firstly, it uses a lot more data to fit the distribution, and secondly, by setting the threshold high enough, the data will be better distributed in time, improving the likelihood that the data samples are independent of each other (one of the conditions of EV applications).

The latter is the method recommended when maximum daily observations are available [1] [46]. One of the problems in fitting the GPD is the selection of the appropriate threshold. Return period calculations using GPD distributions are very sensitive to the threshold selection.

In this study, we use the latter technique and calculate the appropriate threshold u using the automatic procedure developed by Sanabria and Cechet [47].

The parameters of the GPD distribution, location μ_z, scale σ and shape ξ can be calculated from the moment m_z and the second cumulant of Z (κ_2) using the expressions [44] [45],

$$\mu_z = m_z \tag{9}$$

$$\sigma = m_z \left(\left[m_z^2 / \kappa_2 \right] + 1 \right) / 2 \tag{10}$$

$$\xi = \left(\left[m_z^2 / \kappa_2 \right] - 1 \right) / 2 \tag{11}$$

From these parameters the curve of RP follows ([1]), see **Figure 5**,

$$\mathrm{RL}_j = u - \sigma / \xi \left(\left[\mathrm{RP}_j * \mathrm{nopy} * \mathrm{crate} \right] - \xi \right) - 1.0 \tag{12}$$

where,

RL_j is the Return Level corresponding to a given Return Period, RP_j, u is the threshold, nopy is the scale factor and crate is the cross rate or proportion of excesses over the threshold. The y-axis in **Figure 5** is wind speed in m/s.

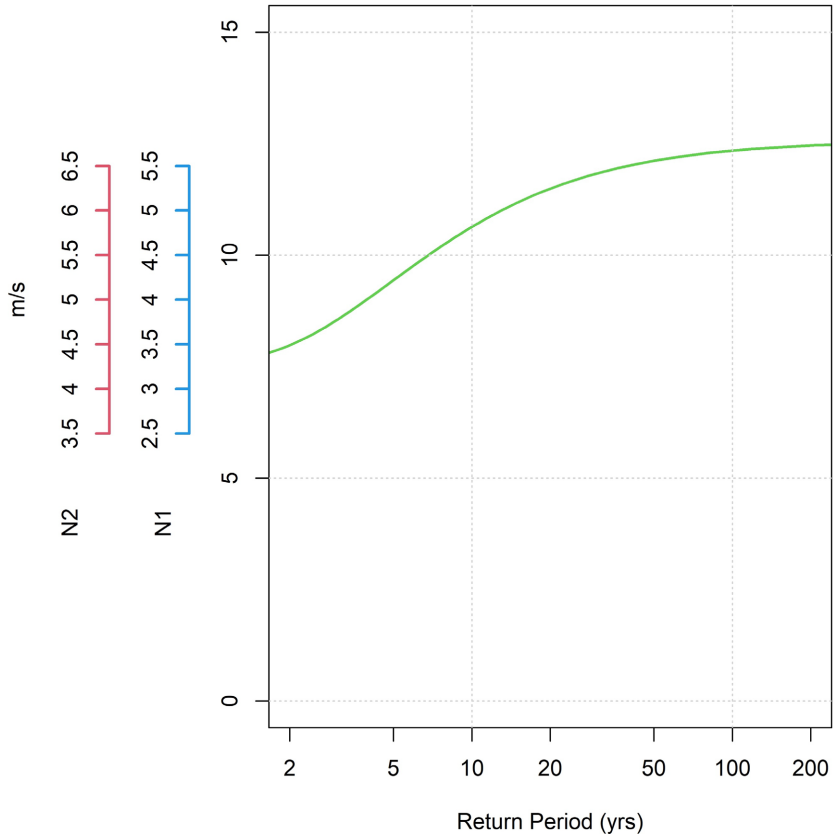

Figure 5. RP of the Compound distribution (Resulting rv Z).

4. Example

As an illustrative example, consider the well-known problem of a landing cyclone near a low-gradient coastal city located on the estuary of a river. In this case, the city is vulnerable to flooding hazards from intense rainfall and the cyclone's coastal storm surge. From a meteorological point of view, at least five drivers impact the hazard: Precipitation, wind speed, sea-level rise, astronomic tide and central pressure [22] [27] [48]-[50].

Wind speed can produce a storm surge, which, combined with sea level, can substantially flood the region with ocean waters, especially at high tide, more so if

sea level rise due to climate change is considered. Furthermore, the river discharge in the sea, which depends on precipitation, can exacerbate the flood hazard in the region. The five drivers referred to above can be collapsed into three climatic variables: Wind speed, which drives the storm surge. Precipitation may flood the area, depending on its magnitude and topography. However, the flooding will likely be due to the heavy river discharge into the sea. The compound effect of the river discharge and storm surge increases the hazard. Finally, the sea level; if the cyclone landing occurs at high tide or the region is already affected by sea level rise due to climate change, the likelihood of the flood increases. The cyclone's central pressure can aggravate the situation. We will use sea level as a proxy for all these complex interactions to simplify the example.

What is essential in this case is to assess the probability that the extremes of the three phenomena, wind, precipitation and sea level, occur concurrently. Very seldom do the peak values of these events coincide; however, the combination of several off-peak extremes can build up to produce a hazardous situation [17]. What is necessary is, then, to calculate the probabilistic distribution of the combined extremes.

Data Description

We acquired data from the Australian Bureau of Meteorology [51] for this illustrative example. For wind, we have maximum daily wind gust in m/s. For precipitation, we have cumulative daily values in mm. In both cases, the data covers the period 2006 to 2019 (14 years). For sea level, we have 40 years of maximum monthly sea level in m (1981-2020). The recorded data stations are located in the same region (greater Sydney). Referring to the three phenomena to a common axis for the cumulant-based convolution process is convenient. This can be achieved by expressing the variables per unit (pu), and dividing each one by the maximum value found in the respective period. **Table 1** shows the maximum value of the three phenomena. **Figure 6** and **Figure 7** show the histogram and density function of the wind speed and precipitation distributions, respectively. For the latter, we have selected values > 4 mm. The histogram and density function of sea level is presented in **Figure 8**. The distributions are assumed to remain static for the study period.

Table 1. Maximum value of the variables used in the example.

Wind speed (m/s)	Precipitation (mm)	Sea level (m)
33.4	106.8	2.3

5. Results

The first step in the calculation of the distribution of the convolution of the three rvs shown in **Figures 6-8**, is to calculate the first moment and the second cumulant of each distribution as explained in Section 3.1. These parameters are presented in **Table 2**. The next step is the calculation of the parameters of the extreme

value distribution that best fits the tail of convolution distribution as explained in Section 3.2 see Figure 4. These parameters are calculated using expressions 8 - 10 and are presented in Table 3. The final step is the calculation of the corresponding curve of RP using Equation (12) as shown in Figure 9.

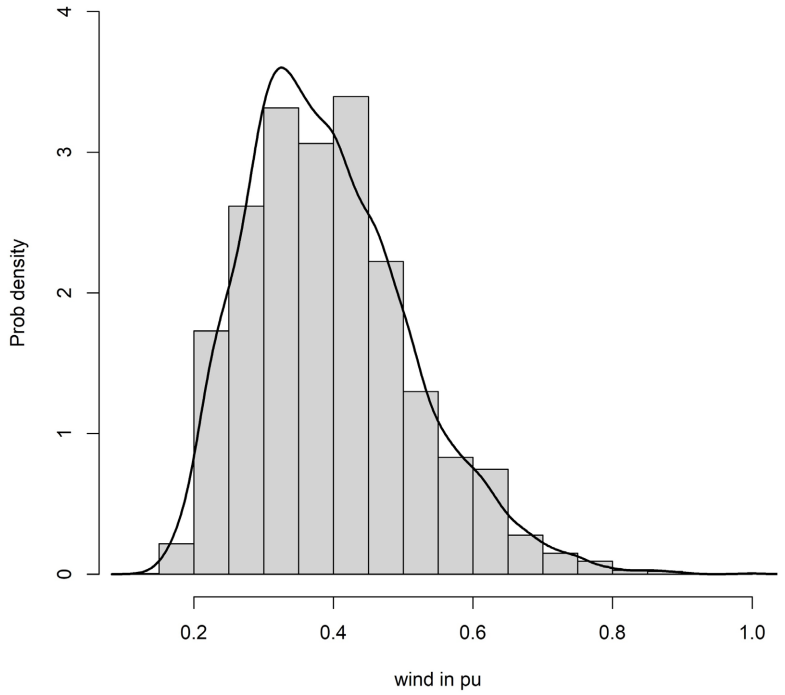

Figure 6. Histogram and density function of wind speed in pu.

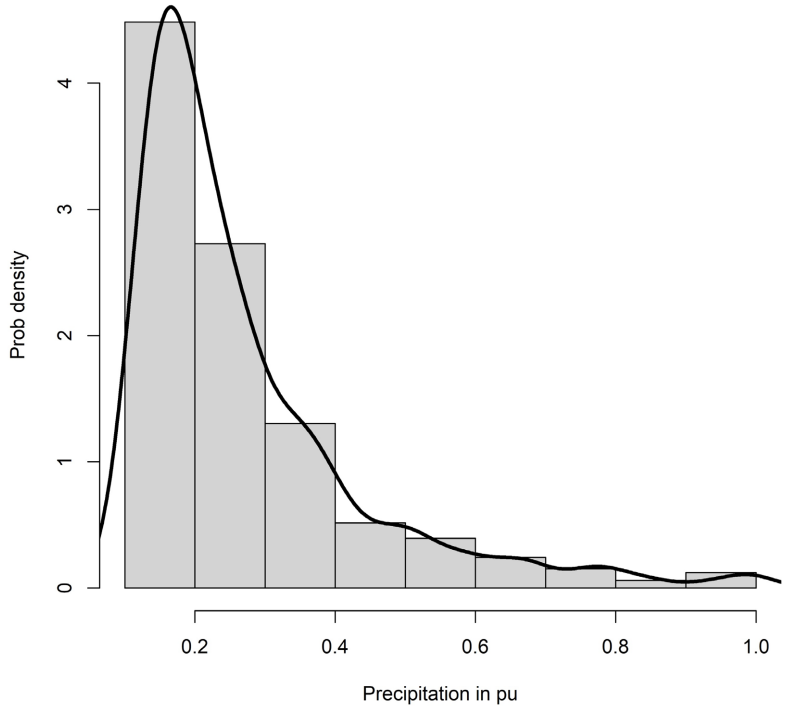

Figure 7. Histogram and density function of precipitation in pu.

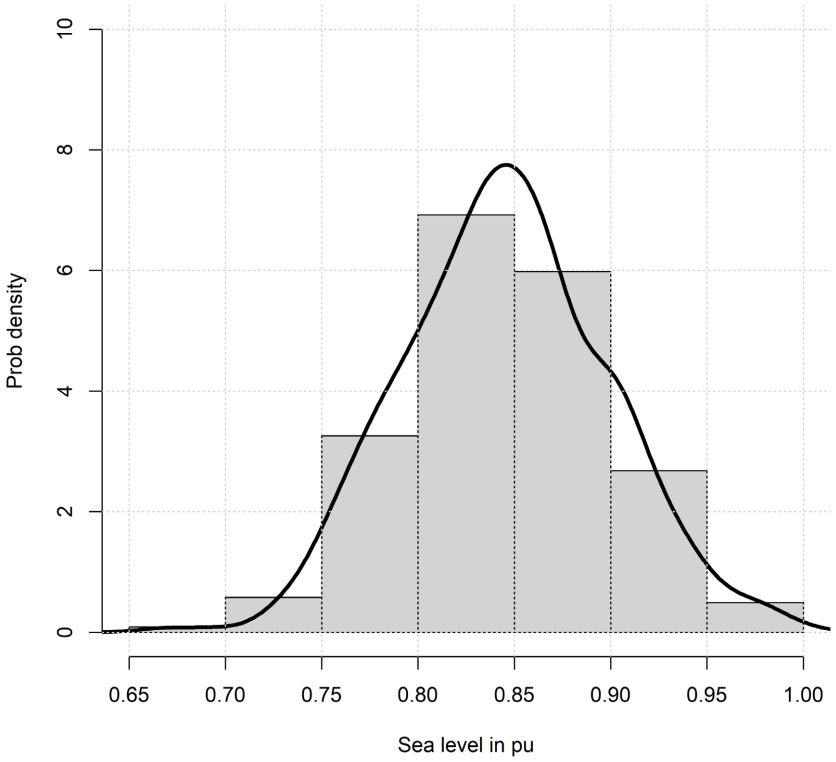

Figure 8. Histogram and density function of sea level in pu.

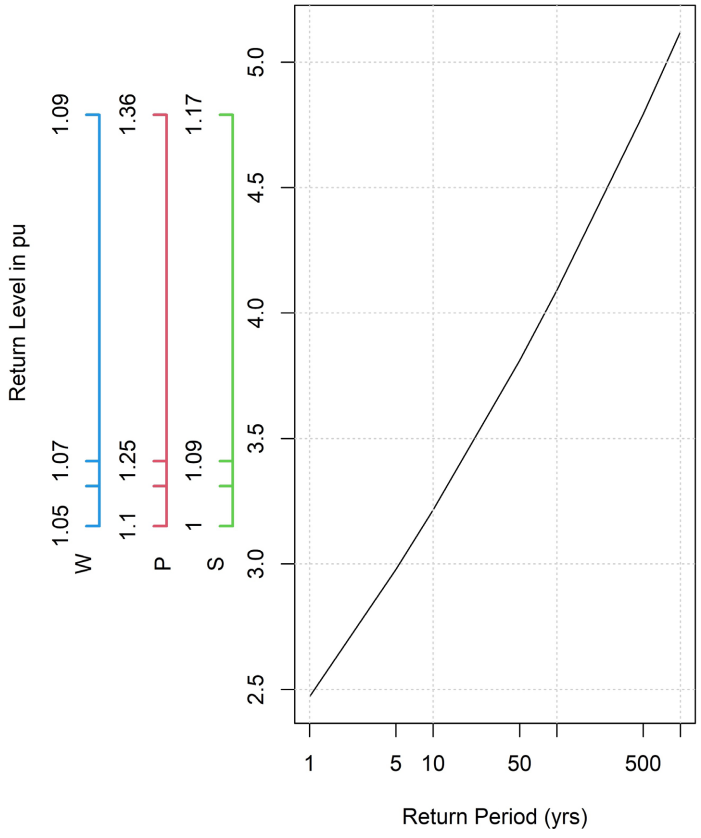

Figure 9. RP of the Compound distribution in pu (all 3 rvs).

Table 2. Parameters of each variable in pu.

Variable	mean (m1)	2nd cumulant (κ_2)	threshold (u)
wind speed	0.394	0.0139	0.475
precipitation	0.270	0.0277	0.300
sea level	0.845	0.0028	0.903
variable Z (convolution)	1.509	0.0445	1.678

Table 3. Parameters of the GPD which best fit the convolution distribution in pu.

mean	location	scale	shape
3.02	1.51	39.43	25.12

Table 4. Covariance between random variables (in pu).

Variable	Wind speed	Precipitation	Sea level
wind speed	-	0.000368	−0.000165
precipitation	0.000368	-	0.000468
sea level	−0.000165	0.000468	-

Figure 9 shows that the compound event wind = 1.05, precipitation = 1.1 and sea level = 1 (first tick mark in the left axes) or in actual units: wind speed = 35.7 m/s, precipitation = 117.5 mm and sea level = 2.32 m can occur, on average, every 9 years. Now, suppose that we know that the compound event wind speed = 36.4 m/s, precipitation = 145.25 mm and sea level = 2.71 m (or in pu: wind = 1.09, precipitation = 1.36 and sea level = 1.17, last tick mark in the left axes) produces a heavy flooding of the city. From the RP curve we can see that the event has a 500-year RP, that is, the city is subjected to these types of flooding, on average, every 500 years; in other words, the annual probability of flooding is very low: 0.002.

Non-Independent rvs

As explained in Section 3.1, the method of cumulants for convolution of rvs can be extended to non-independent rvs by modifying the calculation of the second cumulant. Table 4 shows the covariance of the three rvs used in this example. Compared with the second cumulant (in pu) shown in Table 2, we can see that the covariance is relatively large, and hence, it must be considered for a proper modelling of the problem. The table shows that the covariance is strongest between sea level and precipitation. The positive value shows that the sea level tends to rise with precipitation while decreasing with wind speed.

To compare the curves of RP considering independent and non-independent rvs, both curves have been plotted in a single graph shown in Figure 10. This figure shows that the curve of RP considering non-independence between rvs (red curve) is lower than the one considering independence. For the 100-year RP, the

return level for the former is about 4.75% less than that of the latter. For larger RPs the difference tends to increase. Consider again the compound event wind speed = 36.4 m/s, precipitation = 145.25 mm and sea level = 2.71 m. It used to have a 500-year RP; now it has a 1000-year RP. In other words, considering the covariance between rvs, the event's recurrence happens over a larger interval. This shows the importance of modelling the problem correctly. For mitigation purposes, the overestimation of the RP could result in a substantial increase in the cost.

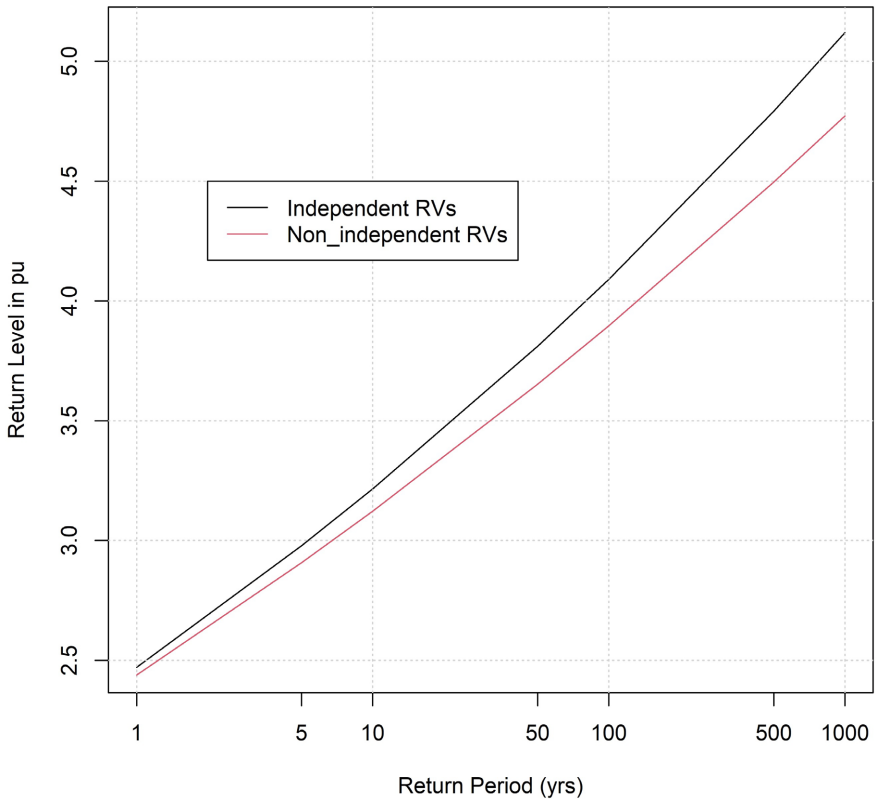

Figure 10. Curve of RP of both independent and non-independent rvs.

6. Conclusions

In this paper, we present a new methodology to assess the probability that extremes of natural phenomena occur concurrently. In the last few years, researchers have recognised that the real danger natural phenomena pose to people and the infrastructure is the extremes of several climatic variables coinciding. In most cases, the peak values of these variables are not coincident; still, other values located in the tail of the distributions can co-occur, leading to a compound extreme, which can result in a catastrophic event. The problem is complicated because the correlation between the climatic variables strongly influences the probability. From the probability of compound events occurring, it is possible to calculate the Return Period, the indicator used to assess hazard and risk in natural phenomena.

Our methodology allows the analyst to deal with any number of correlated

climatic variables in a computationally efficient and mathematically robust way. This facilitates the study of the impact of climate change on natural disasters.

Data and Software

The data used in the example of Section 4 was provided by the Australian Bureau of Meteorology [51]. (Dataset "DC02D_Data_066037_48502949795856.txt"). The tide data was downloaded from "bom.gov.au/australia/tides/". The data processing and figure generation were carried out using the R environment for statistical computing [52].

Conflicts of Interest

The author declares no conflicts of interest regarding the publication of this paper.

References

[1] Coles, S. (2001) An Introduction to Statistical Modeling of Extreme Values. Springer.

[2] Gilleland, E. and Katz, R. (2006) Analyzing Seasonal to Inter-Annual Extreme Weather and Climate Variability with the Extremes Toolkit. 86*th AMS Annual Meeting*, Atlanta GA (USA), 29 January-2 February 2006.

[3] Holmes, J. (2017) Wind Loading of Structures. 3rd Edition, Francis and Taylor.

[4] Palutikof, J.P., Brabson, B.B., Lister, D.H. and Adcock, S.T. (1999) A Review of Methods to Calculate Extreme Wind Speeds. *Meteorological Applications*, **6**, 119-132. https://doi.org/10.1017/s1350482799001103

[5] Seguro, J.V. and Lambert, T.W. (2000) Modern Estimation of the Parameters of the Weibull Wind Speed Distribution for Wind Energy Analysis. *Journal of Wind Engineering and Industrial Aerodynamics*, **85**, 75-84. https://doi.org/10.1016/s0167-6105(99)00122-1

[6] Bousquet, N. and Bernardara, P. (2021) Extreme Value Theory with Applications to Natural Hazards. Springer Nature.

[7] Gumbel, E. (2004) Statistics of Extremes. Dover Publications.

[8] Beirlant, J., Goegebeur, Y., Teugels, J. and Segers, J. (2004) Statistics of Extremes: Theory and Applications. Wiley. https://doi.org/10.1002/0470012382

[9] de Haan, L. and Ferreira, A. (2006) Extreme Value Theory: An Introduction. Springer.

[10] Ranjan, R. and Karmakar, S. (2024) Compound Hazard Mapping for Tropical Cyclone-Induced Concurrent Wind and Rainfall Extremes over India. *NPJ Natural Hazards*, **1**, Article No. 15. https://doi.org/10.1038/s44304-024-00013-y

[11] Bevacqua, E., Vousdoukas, M.I., Zappa, G., Hodges, K.I., Shepherd, T.G., Maraun, D., Mentaschi, L. and Feyen, L. (2020) Global Projections of Compound Coastal Meteorological Extremes. *Natural Hazards and Earth System Sciences*, 1765-1782.

[12] Olmo, M., Bettolli, M.L. and Rusticucci, M. (2020) Atmospheric Circulation Influence on Temperature and Precipitation Individual and Compound Daily Extreme Events: Spatial Variability and Trends over Southern South America. *Weather and Climate Extremes*, **29**, Article ID: 100267. https://doi.org/10.1016/j.wace.2020.100267

[13] Ribeiro, A.F.S., Russo, A., Gouveia, C.M. and Pires, C.A.L. (2020) Drought-related Hot Summers: A Joint Probability Analysis in the Iberian Peninsula. *Weather and Climate Extremes*, **30**, Article ID: 100279. https://doi.org/10.1016/j.wace.2020.100279

[14] Martius, O., Pfahl, S. and Chevalier, C. (2016) A Global Quantification of Compound Precipitation and Wind Extremes. *Geophysical Research Letters*, **43**, 7709-7717. https://doi.org/10.1002/2016gl070017

[15] Huang, W.K., Monahan, A.H. and Zwiers, F.W. (2021) Estimating Concurrent Climate Extremes: A Conditional Approach. *Weather and Climate Extremes*, **33**, Article ID: 100332. https://doi.org/10.1016/j.wace.2021.100332

[16] AghaKouchak, A., Cheng, L., Mazdiyasni, O. and Farahmand, A. (2014) Global Warming and Changes in Risk of Concurrent Climate Extremes: Insights from the 2014 California Drought. *Geophysical Research Letters*, **41**, 8847-8852. https://doi.org/10.1002/2014gl062308

[17] Sutanto, S.J., Vitolo, C., Di Napoli, C., D'Andrea, M. and Van Lanen, H.A.J. (2020) Heatwaves, Droughts, and Fires: Exploring Compound and Cascading Dry Hazards at the Pan-European Scale. *Environment International*, **134**, Article ID: 105276. https://doi.org/10.1016/j.envint.2019.105276

[18] Corbella, S. and Stretch, D.D. (2012) Shoreline Recovery from Storms on the East Coast of Southern Africa. *Natural Hazards and Earth System Sciences*, **12**, 11-22. https://doi.org/10.5194/nhess-12-11-2012

[19] Dowdy, A.J., Mills, G., Finkele, K. and de Groot, W.J. (2009) Australian Fire Weather as Represented by the Mcarthur Forest Fire Danger Index and the Canadian Forest Fire Weather Index. The Centre for Australian Weather and Climate Research, CAWCR Technical Report No. 10. https://www.cawcr.gov.au/technical-reports/CTR_010.pdf

[20] Lucas, C., Hennessy, K., Mills, G. and Bathols, J. (2007) Bushfire Weather in Southeast Australia: Recent Trends and Projected Climate Change Impacts. Bureau of Meteorology Research Centre. Report to the Climate Institute of Australia. http://royalcommission.vic.gov.au/getdoc/c71b6858-c387-41c0-8a89-b351460eba68/TEN.056.001.0001.pdf

[21] French, I., Cechet, R.P., Yang, T. and Sanabria, L. (2013) FireDST: Fire Impact and Risk Evaluation Decision Support Tool. 20*th International Congress on Modelling and Simulation*, Adelaide, 1-6 December 2013, 173-179.

[22] Rahimi, R., Tavakol-Davani, H., Graves, C., Gomez, A. and Fazel Valipour, M. (2020) Compound Inundation Impacts of Coastal Climate Change: Sea-Level Rise, Groundwater Rise, and Coastal Precipitation. *Water*, **12**, Article No. 2776. https://doi.org/10.3390/w12102776

[23] Moftakhari, H.R., Salvadori, G., AghaKouchak, A., Sanders, B.F. and Matthew, R.A. (2017) Compounding Effects of Sea Level Rise and Fluvial Flooding. *Proceedings of the National Academy of Sciences*, **114**, 9785-9790. https://doi.org/10.1073/pnas.1620325114

[24] Vogel, J., Paton, E., Aich, V. and Bronstert, A. (2021) Increasing Compound Warm Spells and Droughts in the Mediterranean Basin. *Weather and Climate Extremes*, **32**, Article ID: 100312.

[25] François, B. and Vrac, M. (2023) Time of Emergence of Compound Events: Contribution of Univariate and Dependence Properties. *Natural Hazards and Earth System Sciences*, **23**, 21-44. https://doi.org/10.5194/nhess-23-21-2023

[26] Stalhandske, Z., Steinmann, C.B., Meiler, S., Sauer, I.J., Vogt, T., Bresch, D.N., *et al.* (2024) Global Multi-Hazard Risk Assessment in a Changing Climate. *Scientific Reports*, **14**, Article No. 5875. https://doi.org/10.1038/s41598-024-55775-2

[27] Xu, H., Xu, K., Bin, L., Lian, J. and Ma, C. (2018) Joint Risk of Rainfall and Storm

Surges during Typhoons in a Coastal City of Haidian Island, China. *International Journal of Environmental Research and Public Health*, **15**, Article 1377. https://doi.org/10.3390/ijerph15071377

[28] Sadegh, M., Moftakhari, H., Gupta, H.V., Ragno, E., Mazdiyasni, O., Sanders, B., *et al*. (2018) Multihazard Scenarios for Analysis of Compound Extreme Events. *Geophysical Research Letters*, **45**, 5470-5480. https://doi.org/10.1029/2018gl077317

[29] Jane, R., Cadavid, L., Obeysekera, J. and Wahl, T. (2020) Multivariate Statistical Modelling of the Drivers of Compound Flood Events in South Florida. *Natural Hazards and Earth System Sciences*, **20**, 2681-2699.

[30] Chen, D., Guo, Y., Zhao, Y., Zhang, J., Liu, X., Tong, Z., *et al*. (2024) Dynamic Evolution Characteristics and Hazard Assessment of Compound Drought/Waterlogging and Low Temperature Events for Maize. *Science of the Total Environment*, **946**, Article ID: 174427. https://doi.org/10.1016/j.scitotenv.2024.174427

[31] Capéraà, P., Fougères, A. and Genest, C. (2000) Bivariate Distributions with Given Extreme Value Attractor. *Journal of Multivariate Analysis*, **72**, 30-49. https://doi.org/10.1006/jmva.1999.1845

[32] Salvadori, G. and De Michele, C. (2010) Multivariate Multiparameter Extreme Value Models and Return Periods: A Copula Approach. *Water Resources Research*, **46**, W10501. https://doi.org/10.1029/2009wr009040

[33] Zscheischler, J., Martius, O., Westra, S., Bevacqua, E., Raymond, C., Horton, R.M., *et al*. (2020) A Typology of Compound Weather and Climate Events. *Nature Reviews Earth & Environment*, **1**, 333-347. https://doi.org/10.1038/s43017-020-0060-z

[34] Guo, Y., Zhang, J., Li, K., Aru, H., Feng, Z., Liu, X., *et al*. (2023) Quantifying Hazard of Drought and Heat Compound Extreme Events during Maize (*Zea mays* L.) Growing Season Using Magnitude Index and Copula. *Weather and Climate Extremes*, **40**, Article ID: 100566. https://doi.org/10.1016/j.wace.2023.100566

[35] Krupskii, P., Joe, H., Lee, D. and Genton, M.G. (2018) Extreme-Value Limit of the Convolution of Exponential and Multivariate Normal Distributions: Link to the Hüsler-Reiß Distribution. *Journal of Multivariate Analysis*, **163**, 80-95. https://doi.org/10.1016/j.jmva.2017.10.006

[36] Kendall, M. and Stuart, A. (1977) The Advanced Theory of Statistics, Volume 1. 4th Edition, Macmillan.

[37] Sanabria, L. (2020) Probabilistic Modelling: An Example-Based Guide. https://www.researchgate.net/publication/371950030_Probabilistic_Modelling_An_example-based_guide

[38] Abella, D.J. and Ahn, K. (2024) Investigating the Spatial and Temporal Characteristics of Compound Dry Hazard Occurrences across the Pan-Asian Region. *Weather and Climate Extremes*, **44**, Article ID: 100669. https://doi.org/10.1016/j.wace.2024.100669

[39] Gnedenko, B.V. (1978) The Theory of Probability. MIR Publishers.

[40] Hirschman, I.I. and Widder, W.D (2005) The Convolution Transform. Dover Publications. https://www.probabilitycourse.com/

[41] Pishro-Nik, H. (2014) Introduction to Probability, Statistics, and Random Processes. Kappa Research LLC.

[42] Lashgari, A., Rahimi, L., Ahmadisharaf, E. and Barari, A. (2024) Probabilistic Pre-Conditioned Compound Landslide Hazard Assessment Framework: Integrating Seismic and Precipitation Data and Applications. *Landslides*. https://doi.org/10.1007/s10346-024-02371-0

[43] Australian/New Zealand Standard (2011) Structural Design Actions. Part 2: Wind Actions. Technical Report, Australian/New Zealand Standard. https://archive.org/details/as-nzs.1170.2.2011

[44] Hosking, J.R.M. and Wallis, J.R. (1987) Parameter and Quantile Estimation for the Generalized Pareto Distribution. *Technometrics*, **29**, 339-349. https://doi.org/10.1080/00401706.1987.10488243

[45] Oztekin, T. (2005) Comparison of Parameter Estimation Methods for the Three-Parameter Generalised Pareto Distribution. *Turkish Journal of Agriculture and Forestry*, **29**, 419-428.

[46] Holmes, J.D. and Moriarty, W.W. (1999) Application of the Generalized Pareto Distribution to Extreme Value Analysis in Wind Engineering. *Journal of Wind Engineering and Industrial Aerodynamics*, **83**, 1-10. https://doi.org/10.1016/s0167-6105(99)00056-2

[47] Sanabria, L. and Cechet, R. (2007) A Statistical Model of Severe Winds. Geoscience Australia, GeoCat No. 65052. https://www.ga.gov.au/bigobj/GA10911.pdf

[48] Santiago-Collazo, F.L., Bilskie, M.V. and Hagen, S.C. (2019) A Comprehensive Review of Compound Inundation Models in Low-Gradient Coastal Watersheds. *Environmental Modelling & Software*, **119**, 166-181. https://doi.org/10.1016/j.envsoft.2019.06.002

[49] Rousseau-Rizzi, R., Raveh-Rubin, S., Catto, J.L., Portal, A., Givon, Y. and Martius, O. (2024) A Storm-Relative Climatology of Compound Hazards in Mediterranean Cyclones. *Weather and Climate Dynamics*, **5**, 1079-1101. https://doi.org/10.5194/wcd-5-1079-2024

[50] Owen, L.E., Catto, J.L., Stephenson, D.B. and Dunstone, N.J. (2021) Compound Precipitation and Wind Extremes over Europe and Their Relationship to Extratropical Cyclones. *Weather and Climate Extremes*, **33**, Article ID: 100342. https://doi.org/10.1016/j.wace.2021.100342

[51] Australian Bureau of Meteorology (2022) Climate Data Services. http://www.bom.gov.au/climate/data/

[52] R Core Team (2022) R: A Language and Environment for Statistical Computing. R Foundation for Statistical Computing. https://www.r-project.org/